

Measurements of solar diurnal anisotropy with GRAPES-3 experiment

P.K. Mohanty^{*a,b}, H.M. Antia^{a,b}, K.P. Arunbabu^{a,b}, S.R. Dugad^{a,b}, S.K. Gupta^{a,b}, B. Hariharan^{a,b}, Y. Hayashi^{d,b}, P. Jagadeesan^{a,b}, A. Jain^{a,b}, S. Kawakami^{d,b}, H. Kojima^{f,b}, S.D. Morris^{a,b}, P.K. Nayak^{a,b}, T. Nonaka^{d,b}, A. Oshima^{e,b}, B.S. Rao^{a,b}, S. Shibata^{e,b}, P. Subramanian^{c,b}, K. Tanaka^{g,b}

^aTata Institute of Fundamental Research, Mumbai 400 005, India.

^bThe GRAPES-3 Experiment, Cosmic Ray Laboratory, Raj Bhavan, 643 001 Ooty, India.

^cIndian Institute of Science Education and Research, Pune 411 021, India.

^dGraduate School of Sciences, Osaka City University, Osaka 558-8585, Japan.

^eCollege of Engineering, Chubu University, Kasugai, Aichi 487-8501, Japan.

^fFaculty of Engineering, Aichi Institute of Technology, Toyota City, Aichi 470-0392, Japan.

^gGraduate School of Information Sciences, Hiroshima City University, Hiroshima 731-3194, Japan.

Email: pkm@tifr.res.in

Harmonics in the cosmic ray solar diurnal anisotropy up to third have been experimentally observed. Very high statistics is required to investigate higher harmonics because of exceedingly small amplitudes. The GRAPES-3 experiment located in Ooty, India contains a large area (560 m²) tracking muon telescope that provides a high statistical record of the muon flux ($\sim 4 \times 10^9$ per day). This allows measurement of tiny variations in cosmic ray intensity ($\lesssim 0.01\%$) caused by various solar phenomena. After making appropriate corrections for the efficiency of the detector and atmospheric pressure variations, a continuous stream of one year data was used to investigate the diurnal anisotropy. A fast Fourier transform based analysis revealed clear presence of the first three harmonics as well as a fourth harmonic for the first time. Further, a clear rigidity dependence of each of the four harmonics was also obtained. These results are presented in this paper.

*The 34th International Cosmic Ray Conference,
30 July- 6 August, 2015
The Hague, The Netherlands*

*Speaker.

1. Introduction

After correcting for the atmospheric pressure variations, the flux of secondary cosmic ray particles such as neutrons and muons recorded by ground based detectors exhibits a periodic variation related to a solar day. The amplitude of this variation is typically about 0.3–0.4% observed by neutron monitors and about 0.1–0.2% observed by muon detectors. This phenomena which is referred as solar diurnal anisotropy is explained generally by the convection of particles outward by solar wind and the inward diffusion along the interplanetary magnetic field (IMF). The balance of these two effects produces a net anisotropic flow of galactic cosmic rays along the orbital direction of the motion of the Earth. During a solar day, when the detector views the flow direction, a maximum intensity is observed while a minimum intensity is observed in the opposite direction [1]. Several quantitative information such as scattering mean free path and diffusion coefficients in the interplanetary medium can be derived using the measured parameters of diurnal anisotropy such as amplitude, phase and rigidity dependences [2]. In addition to the fundamental period of 24 h, observations have established the existence of higher harmonics in the diurnal anisotropy up to third [3, 4]. However, so far there are no accepted theoretical models that could adequately explain the origin of all the higher harmonics. In view of the exceptionally high statistics and narrow angle measurements offered by the large area (560 m²) GRAPES-3 tracking muon detector, an attempt was made to investigate this phenomena in detail as described in the following sections.

2. THE GRAPES-3 EXPERIMENT

The GRAPES-3 experiment is located at Ooty in South India (11.4°N latitude, 76.7°E longitude and 2200 m altitude). It comprises of an array of ~ 400 plastic scintillator detectors of area 1 m² each with 8 m inter-detector separation and a large area (560 m²) tracking muon detector [5, 6]. The muon detector consists of 16 separate modules of 35 m² area each. Four layers of proportional counter (PRC) tubes (58×4 numbers) each of length 6 m and cross section 10 cm \times 10 cm, arranged in two orthogonal planes allows to track the passage of muons and determine their arrival directions in 13×13 (169) directional bins. A total thickness of 550 g cm⁻² of absorber in form of concrete blocks above the bottom layer of the PRCs allows detection of penetrating muons above a threshold energy of 1 GeV. The high count rate of muons (~ 3000 s⁻¹) recorded in 13×13 (169) directional bins in each module allows to make sensitive measurements on various solar phenomena including Forbush decreases associated with coronal mass ejections [7, 8], diurnal and sidereal anisotropies [9, 10].

3. Harmonic Analysis and Results

In this analysis, we used the time series muons rates (4 min average) from 1 January to 31 December 2006. Various instrumental effects in the data such as gaps, spikes, jumps in the rates and fluctuations were identified through visual inspections and these periods of data were excluded for further analysis. Apart from the short lived variations, the data also exhibit gradual, but small efficiency variations which were caused primarily due to the gain variation of PRCs. These variations were modeled by fourth order polynomial fits and corrected [11]. Thereafter, the data from the 16

modules were combined together to improve the statistical accuracy and minimize the gaps. After the efficiency corrections, the data contains either atmospheric or solar effects. The atmospheric pressure effects were corrected using an accurate value of pressure coefficient. The determination of the pressure coefficient was made using a fast Fourier technique (FFT) which is discussed in a separate paper in this conference. To perform the FFT analysis, a total of 2^{17} , 4 minute successive intervals of data spanning over 364.12 days starting from 1 January 2006 was used. The percent deviation of each 4 min rates from the yearly mean was calculated. The gaps in the data which constituted only less than 0.1% distributed throughout were padded with zeros. Fig. 1 shows the FFT spectrum of the vertical direction. The harmonic peaks of the diurnal anisotropy at frequencies 1, 2, 3 and 4 cycles per day (cpd) were clearly observed in the FFT spectrum.

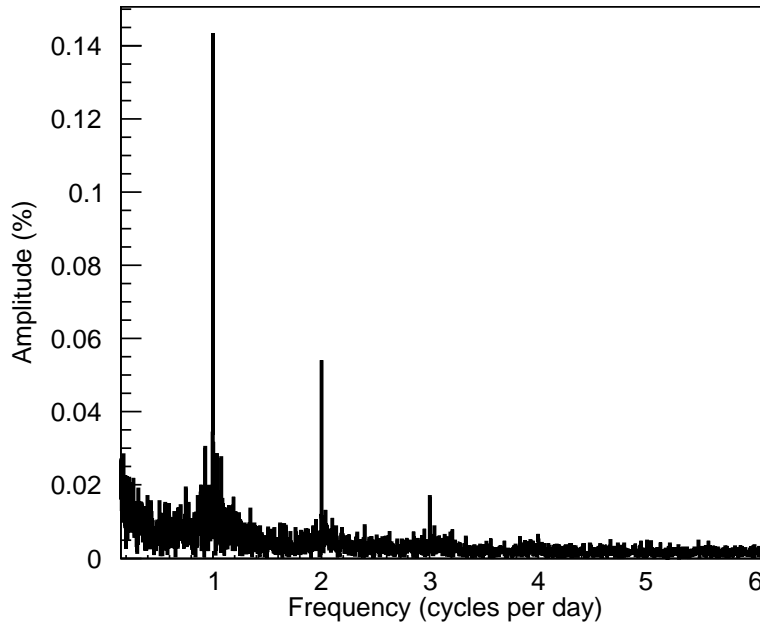


Figure 1: FFT spectrum of muon data for the vertical directional bin of the GRAPES-3 muon detector corresponding to a median rigidity value of 66 GV.

A quantitative understanding of the diurnal anisotropy may be attempted by studying the rigidity dependence of the harmonic amplitudes and phases. For this purpose it was essential to calculate the median rigidity of the primary cosmic rays (PCRs) responsible for the production of muons detected in each direction of the GRAPES-3 muon telescope. The cutoff and median rigidity values for each the 169 were calculated taking into the effect of geomagnetic bending using a trajectory program [12] and the standard geomagnetic field model called the International Geomagnetic Reference Field 11th generation (IGRF-11)" [13]. Atmospheric simulation of primary protons were performed using air shower simulation code CORSIKA [14]. An in-house developed program was used to simulate detector response taking into the geometrical factors of the detector and various experimental trigger criteria. The calculated cutoff rigidity varied from a minimum value of 14 GV from a West direction to a maximum value of 32 GV in a East direction bin across the 169 directional bins. The calculated median rigidity values varied from 64 GV to 141 GV.

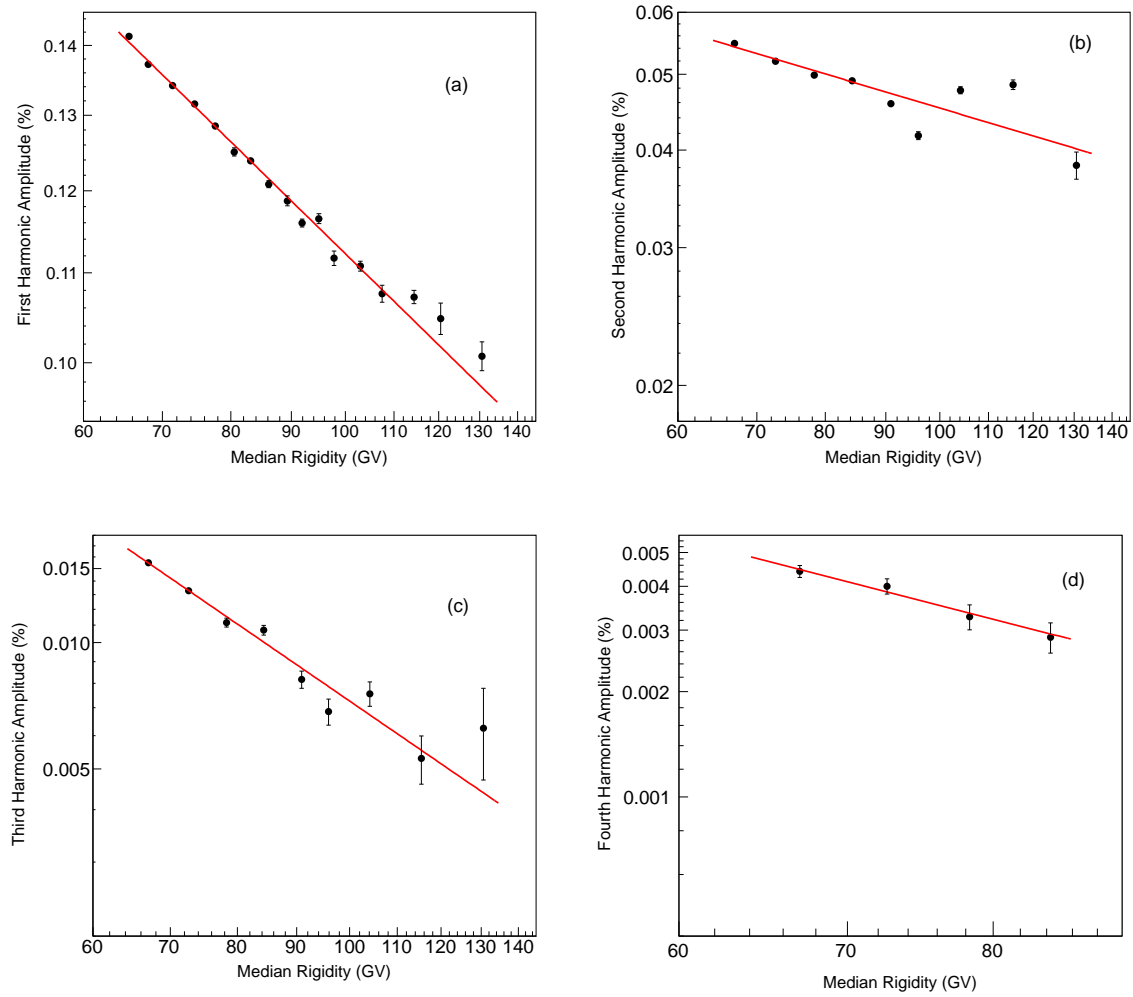


Figure 2: Rigidity dependence of harmonic amplitudes of diurnal anisotropy measured using 2006 data for (a) first harmonic, (b) second harmonic (c) third harmonic, and (d) fourth harmonic. Both x and y-axis are shown in log scale. The red solid lines represent the power law fit of the form $K \times R_m^\gamma$, R_m is the median rigidity.

Data from several directional bins were combined to increase the statistics and hence reduce the background amplitude in the FFT spectrum. The data of 169 directional bins were classified into 17 rigidity bins to investigate first harmonics and 9 rigidity bins for second, third and fourth harmonics. Time offsets due to the Earth's rotation were corrected to align the data of different directions to the vertical direction using the angle of each direction determined from the geometrical alignment of the PRCs in the four layers in the module. Next, the data of different directional bins constituting a rigidity bin were combined and FFT analysis was performed. Fig.2 shows the rigidity spectra for the four harmonics. The rigidity dependence of the amplitudes were derived by fitting a power law of the form $K \times R_m^\gamma$, where R_m was the median rigidity and γ the spectral index. Clearly, time offset corrected data provided good fits for each of the four harmonics displaying an

inverse correlation of the amplitude with the rigidity. The spectral slopes obtained from the fits for the first, second, third, and fourth harmonics were (-0.531 ± 0.006) , (-0.45 ± 0.02) , (-1.89 ± 0.08) , and (-1.8 ± 0.4) , respectively. The small values of error on the spectral indices clearly underline the very high statistical significance of these measurements.

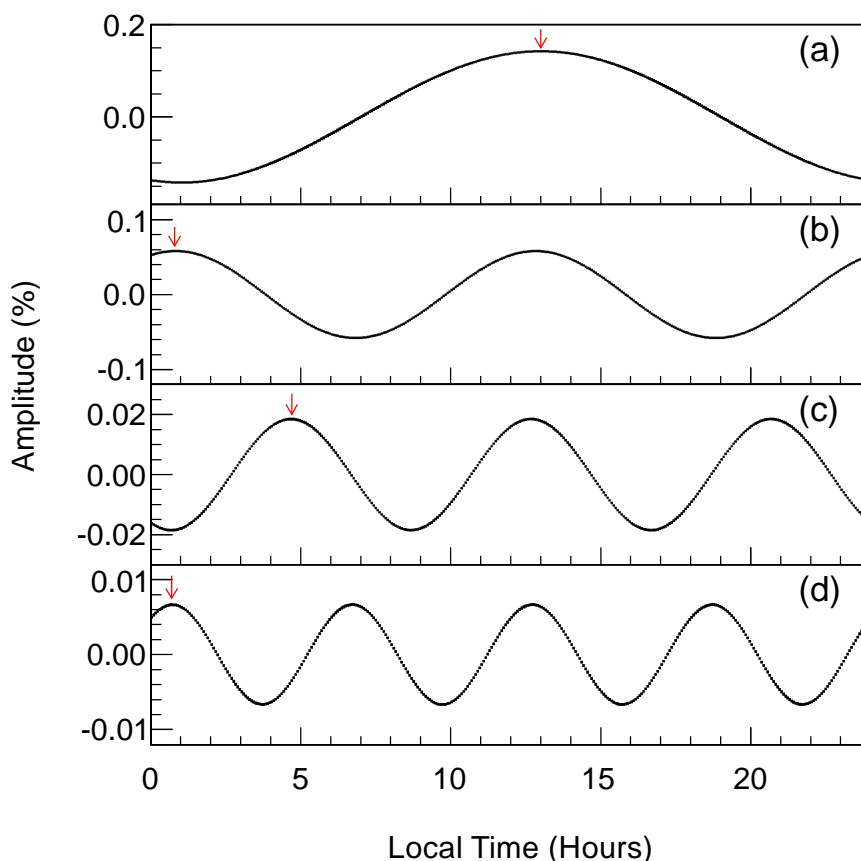


Figure 3: Time domain data after IFFT, folded modulo 24 h for rigidity bin 64–70 GV, (a) first (b) second (c) third, and (d) fourth harmonic. Phase of each harmonic corresponded to the local time of first maximum indicated by pointers.

Besides its amplitude, the phase of the diurnal anisotropy is another important parameter that is related to its direction. To obtain the phase of each rigidity bin for a harmonic peak, the corresponding FFT spectrum was selected using the narrow band pass filter and then an inverse FFT was performed. The resultant time domain data were folded modulo 24 h. This is illustrated in Fig. 3 for all four harmonics for rigidity bin 64–70 GV. The phase was defined as the local time of the first maximum of the anisotropy during 24 h. It was observed that the phases were very similar for different rigidity intervals. The mean and the root mean square (rms) values of the phases for various rigidity bins for the first, second, third, and fourth harmonics were (12.4 ± 0.3) h, (0.4 ± 0.3) h, (4.7 ± 0.2) h and (0.9 ± 0.2) h local time, respectively. It is interesting to note that the phases of four harmonics became nearly same if integral multiples of periods, namely, 12 h, 8 h and 2×6 h are added to the second, third, and fourth harmonic. The phase values became (12.4 ± 0.3) h, (12.7 ± 0.2) h and (12.9 ± 0.2) h in close agreement with the phase of first harmonic.

4. Summary

A comparison of the amplitudes of the first three harmonics from our observations provided good agreement with the results reported by others in the past. Further, the unambiguous observation of a fourth harmonic is new and unique. The rigidity spectrum of harmonics over a wide range of rigidities with extremely high significance was measured for the first time using a single detector, namely, GRAPES-3. The observation of a similar phase for all four harmonics showed that these features could not be due to different physical processes. Our results strongly support the class of models proposed by Owens [15], and by Bieber & Pomerantz [16] that allow generation of harmonics higher than second harmonic and the higher harmonics were believed to be manifestation of a common physical process. In light of these sensitive measurements, a good theoretical framework for the interpretation of these results would be extremely useful in obtaining valuable information on cosmic ray transport in the interplanetary medium and the dynamics of the electromagnetic environment of interplanetary space. Several solar modulation parameters such as the mean scattering free path and diffusion coefficients in the heliosphere can be derived using these measurements. Work is in the progress to convert the observed anisotropy to space anisotropy outside the magnetosphere of the Earth.

References

- [1] E. N. Parker, *Planet. Space Sci.* **12** (1964) 735.
- [2] K. Munakata et al., *The Astrophysical Journal* **791:22**(16pp) (2014).
- [3] K. Nagashima et al., *Proc. 15th ICRC, Plovdiv*, **4** (1977) 72.
- [4] H. S. Ahluwalia and M. M. Fikani, *J. Geophys. Res.* **101** (1996) 11075.
- [5] S. K. Gupta et al., *Nucl. Instrum. Meth. A* **540** (2005) 311.
- [6] Y. Hayashi et al., *Nucl. Instrum. Meth. A* **545** (2005) 643.
- [7] T. Nonaka et al., *Phys. Rev. D* **74** (2006) 052003.
- [8] K. P. Arunbabu et al., *Astron. Astrophys.*, **555** (2013) A139.
- [9] P. K. Mohanty et al., *Pramana - J. Phys.* **81** (2013) 343.
- [10] H. Kojima et al., *Astroparticle Phys.* **62** (2015) 21.
- [11] S. K. Gupta, *EPJ Web of Conferences* **52** (2013) 04005.
- [12] D. F. Smart et al., *Space Sci. Rev.* **93** (2000) 305.
- [13] C. Finlay et al., *Geophys. J. Int.* **183** (2010) 1216.
- [14] <http://www-ik.fzk.de/corsika>.
- [15] A. J. Owens et al., *Astrophys. J.* **243** (1981) 322.
- [16] J. W. Bieber and M. A. Pomerantz, *Geophys. Res. Lett.* **10** (1983) 920.